

## The Effect of Geometrical Transitions on the Wave Overtopping Load

Vera M. van Bergeijk<sup>(1)</sup>, Jord J. Warmink<sup>(1)</sup> and Suzanne J.M.H. Hulscher<sup>(1)</sup>

<sup>(1,3)</sup> University of Twente, Enschede, The Netherlands

v.m.vanbergeijk@utwente.nl, j.j.warmink@utwente.nl, s.j.m.h.hulscher@utwente.nl

### Abstract

Erosion by overtopping waves can lead to failure of grass-covered earthen flood defences. Previous studies have indicated that cover failure starts at changes in material or geometry defined as transitions. In this study, the overtopping flow at geometrical transitions is modelled and their effect on the hydraulic load is quantified. A numerical model is developed in the OpenFOAM software and simulates the overtopping flow over the crest and the landward slope of a grass-covered flood defense. Two types of geometrical transitions were studied: slope changes and height differences. These transitions are representative for the landward crest line, the landward toe, erosion holes on the slope and a road on the crest. New relations are developed for the maximum shear stress and the maximum normal stress as result of the geometrical transitions using design parameters such as the geometry and the overtopping volume. These relations can be used in existing calculation methods to include the effects of geometrical transitions on the hydraulic load for the design and the safety assessment of flood defences.

**Keywords:** OpenFOAM; Modelling; Erosion; Height transition; Slope change

### 1. INTRODUCTION

Wave overtopping is one of main failure mechanism of flood protective structures (Figure 1). Dikes – grass-covered earthen flood defences – and earthen dams are found all over the world to protect the hinterland from flooding. More extreme weather conditions and sea level rise due to climate change may result in more frequent overtopping at many locations all over the world. Especially structures with an earthen cover are vulnerable for climate change because droughts decrease the strength of the vegetation and cover material. This calls for cover designs that are more erosion resistant for wave overtopping.

Observation, experiments and numerical simulations have indicated that failure of the cover layer starts at transitions (Simm et al., 2021; Bomers et al., 2018; Steendam et al., 2014). Transitions are defined as any change in cover material or geometry. These transitions are vulnerable locations for cover failure since they affect the hydraulic load and the strength of the cover. Therefore, the effects of transitions need to be included in the calculation methods for the design and the assessment of flood defences.



**Figure 1:** Locations of dike and dam failures reported in the International Levee Performance Database (Özer et al., 2020), hydraulic failures of earthen dams and embankments as the result of overtopping based on

Talukdar & Dey (2019) and locations of wave overtopping field test (Frankena, 2019). Adapted from Van Bergeijk (2022)

The hydraulic forces on the cover are required to determine the stability and the erosion resistance of the cover. Field tests and physical model tests in wave flumes and basins are performed to determine the strength of flood defences against wave overtopping. During these tests, the average overtopping discharge and the overtopping flow velocity can be measured. However, other hydraulic variables such as the pressure, the shear stress and the normal stress are necessary to describe the failure process (Zhang et al., 2017; Schüttrumpf & Oumeraci, 2005). These can not be measured during tests, but computational fluid dynamics CFD models can provide information on these variables. Several CFD models have been used to simulate the hydraulic load by waves on coastal structures with a hard revetment (Chen et al., 2021; Altomare et al., 2015) porous medium (Barendse et al., 2022; Palma et al., 2019) or grass cover (Van Bergeijk et al., 2020; Bomers et al., 2018). These models provide information on the spatially and temporal variation in the hydraulic variables and can be used to study the load on the cover by overtopping waves.

Geometrical transitions include slope changes, such as the transition from the crest to the landward slope, and cliffs that can form at erosion holes (Figure 2). Field tests and numerical models have shown that these geometrical transitions lead to flow separation resulting in high impact forces at the location of reattachment (Van Bergeijk et al., 2022; Ponsioen et al., 2019; Van Damme et al., 2016). These impact forces can explain why geometrical transitions are vulnerable for cover erosion. These forces need to be quantified so the additional load as the result of geometrical transitions can be included in existing calculation methods for wave overtopping.

The goal of this paper is to quantify the effects of geometrical transitions on the hydraulic load of overtopping waves. A numerical model is used to compute the hydraulic load as the result of geometrical transitions. Relations for the load are developed that can be used in existing erosion models to include the effect of transitions in the design and assessment of flood defences. Two types of geometrical transitions are studied: slope changes and height transitions. The hydraulic load due to the slope change at the landward crest line and the landward toe is studied. Additionally, height transitions on the crest representative for a road are studied as well as height transitions on the landward slope representative of an erosion hole.

The paper is organized as follows: Section 2 describes the numerical model set-up and the processes observed in the numerical model. Relations for the hydraulic load at geometrical transitions are developed in Section 3. Section 4 describes the application of the new relations and the conclusions are drawn in Section 5.



**Figure 2:** Photos of height transitions: (a) Height difference between the grass cover and asphalt at a roadside (Photo by Vera van Bergeijk), (b) Vertical cliff formed at an erosion hole (Bakker et al., 2008).

## 2. NUMERICAL SIMULATION OF THE OVERTOPPING FLOW

### 2.1 Numerical Model Set-Up

We developed a numerical model to simulate the overtopping flow over the crest and the landward slope of a grass-covered flood defence. The model uses the CFD software OpenFOAM® to solve the Reynolds-Averaged Navier Stokes equations. The turbulence is solved using a  $k-\omega$  SST turbulence model and a Nikuradse roughness height of 8 mm was used to include the roughness of the grass cover. A full description of the model and the model validation can be found in Van Bergeijk et al. (2020) and Van Bergeijk et al. (2022).

The model domain is 2D vertical with grid sizes of 1 cm x 1 cm (horizontal x vertical). Four grids were created to simulate the four cases (Table 1, Figure 3): (1) normal dike profile with a steep landward slope, (2)

dike profile with an erosion hole on a gentle landward slope, (3) dike profile with a road on top of the crest that is located lower than the surrounding grass vegetation and (4) a dike profile with a road on top of the crest that is located higher than the surrounding grass vegetation. The goal of this paper is to study solely the effects of geometric transitions and therefore a uniform grass cover is used for all cases. In reality, the bed roughness changes for clay in erosion holes and asphalt for roads. However, previous studies have shown that the change in roughness only has a limited effect on the hydraulic load (Van Bergeijk, 2022; Van Bergeijk et al., 2020b; Bomers et al., 2018).

The model output includes the flow velocity, the shear stress, the normal stress and the pressure as function of time and location. The shear stress describes the wall shear stress parallel to the dike profile and the normal stress describes the wall shear stress perpendicular to the dike profile. Simulations with an overtopping volume of  $2.0 \text{ m}^3/\text{m}$  are performed to study the overtopping flow over the geometric transitions and identify locations of flow separation and reattachment to the dike cover.

**Table 1:** Geometry of the four cases

Case	Crest width [m]	Slope steepness	Slope length [m]	Height transition [cm]	Source
1	3	1:1.7	6	-	Van Bergeijk et al. (2022)
2	7	1:2.7	18	40	(Van Bergeijk et al., 2021)
3	7	1:2.7	-	10	Van Bergeijk (2022)
4	7	1:2.7	-	10	Van Bergeijk (2022)

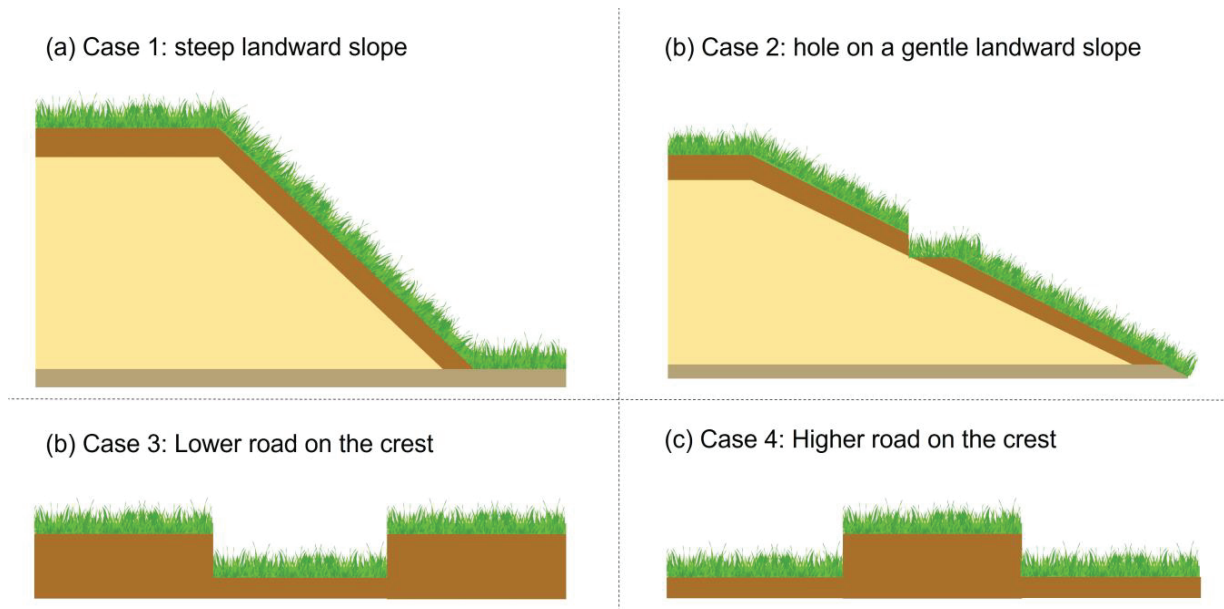


**Figure 3:** Schematization of the four cases.

## 2.2 Model Results

Figure 4 shows snapshots of the model simulations where the flow separation is clearly observed for all four cases. For the first case, the steep landward slope results in a large slope change and therefore the flow separates at the landward crest line. This leads to high normal stresses and pressures on the upper slope at the location of reattachment (red dashed circle in Figure 4a). The pressure, the flow velocity and the shear stress are maximal around 0.5-1m landward of the toe. This maximum is the result of high flow velocities at the end of the slope and additional turbulence created by the slope change.

The second case is a height transition on a gentle landward slope. In this case, no flow separation occurs at the landward crest line due to the smaller slope change for a gentle slope. However, the flow separates at the vertical drop of the hole and reattaches in the hole (Figure 4b). This results in a high normal stress and shear stress at the location of reattachment.

Case 3 includes two height transitions: a vertical drop and a vertical rise. The flow separates at the vertical drop similar to the erosion hole. When the flow reaches the vertical rise, the flow sweeps up in the air, travels to the air and impacts at the end of the crest and on the upper slope (Figure 4c). The shear stress and normal stress increase at both reattachment locations, but the stresses are maximal as result of the vertical

rise. This is because the flow sweeps around 0.5-1m into the air followed by a drop of this height leading to higher impact forces compared to the first drop of 10 cm. Additionally, the impact against the vertical rise results in high peak pressures at this location, similar to the impact of the overtopping flow against a vertical wall.

The fourth case also includes two height transitions: first a vertical rise followed by a vertical drop. Similar to the third case, the flow sweeps up in the air at the vertical rise leading to high stresses at the location of reattachment. The flow also separates at the vertical drop, but the stresses at the impact location are smaller compared to the vertical rise.

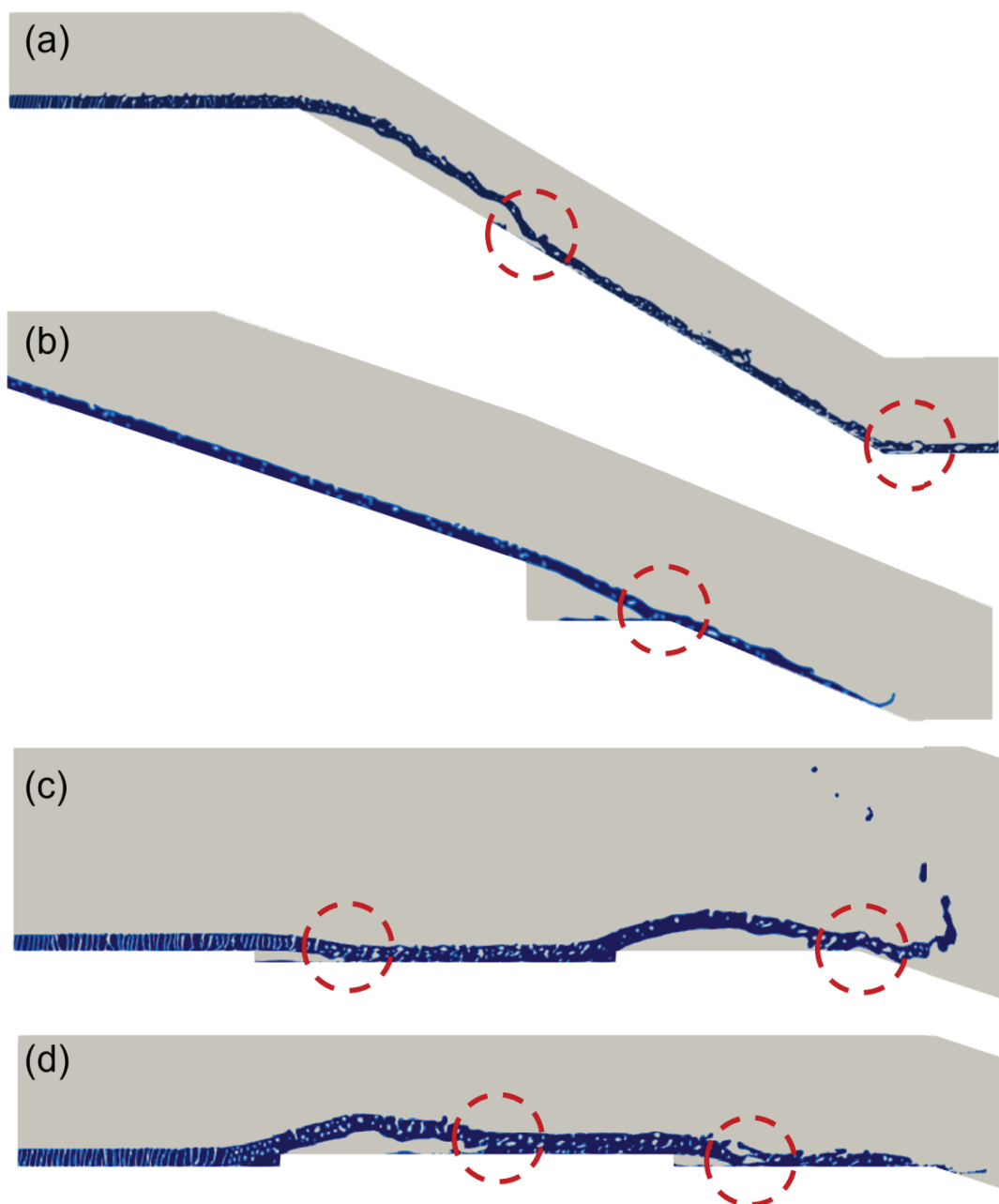


**Figure 4:** Snapshot of the model results where blue indicates water and gray indicates air. The red dashed circles indicate locations of high hydraulic loads. (a) Transitions in slope at the landward crest line and the landward toe. (b) A height transition on the slope comparable to an erosion hole. (c) A road on the crest that is located lower than the grass cover. (d) A road on the crest that is located higher than the grass cover.

### 3. THE HYDRAULIC LOAD AT TRANSITIONS

Existing erosion models for cover erosion that include the effects of the transitions use the flow velocity to describe the hydraulic load (Van Bergeijk et al., 2021; Van Der Meer et al., 2010). Transitions in cover type mainly affect the overtopping flow velocity and their effect can be calculated using analytical formulas for the overtopping flow velocity (Van Bergeijk et al., 2019; Schüttrumpf & Oumeraci, 2005). Ponsioen et al (2019) developed analytical formulas for the normal stress based on the flow velocity as result of the flow separation at the crest line. However, no analytical or empirical formulas are available for other geometric transitions and therefore these transitions can not be included in existing erosion models used for the design and safety assessments of flood defences.

In this section, relations for the hydraulic load at the geometric transitions using the numerical model. A model study is performed wherein the main design parameters are varied. The effect of the design parameters on the load are quantified using a regression analysis as described by Chen et al. (2020) and Van Bergeijk et al. (2022). For all four cases, the overtopping volume  $V$  is varied since this parameter determined the amount of water flowing over the crest. The steepness  $\cot(\varphi)$  and the length  $L$  of the landward slope are also varied for the load at slope changes (Case 1, Figure 3). The height of the transition  $d$  is varied for the height transitions on the slope (Case 2) and height transitions on the crest (Cases 3 and 4).

#### 3.1 The Effect of Slope Changes

For grass-covered flood defences, the maximum hydraulic load occurs as the result of slope changes. The load is maximum at the landward toe for flood defences with a gentle slope ( $\cot(\varphi) > 3$ ). The maximum load at this location is described by the shear stress  $\tau_s$  and depends on the overtopping volume, the flow velocity on the crest  $U_0$ , the length of the landward slope and the steepness of the landward slope (Figure 5a)

$$\tau_{s,toe} = 22.7 \frac{U_0^2 \sqrt{VL}}{\cot \varphi^3} + 708 \quad [1]$$

The shear stress and the normal stress have the dimensions  $N/m^2$  and therefore the coefficients of the fits have the dimensions  $22.7 \text{ kg/m}^{9/2}$  and  $708 \text{ N/m}^2$ . The fit has a coefficient of determination  $R^2$  of 0.70. The positive offset indicates that each overtopping wave exerts a shear stress at this location.

In case of steep landward slopes and large overtopping volumes, the wave can separate at the landward crestline and impacts on the upper slope. This impact results in a high normal stress  $\tau_n$  at the location of reattachment  $X$ . The normal stress and reattachment location depend on the conditions on the crest and the upper slope, and are therefore not affected by the slope length  $L$  (Figures 5b and 5c).

$$\tau_{n,crestline} = 75.8 \frac{U_0^2 V^{1/5}}{1.5 + \cot \varphi} - 156 \quad [2]$$

$$X = 6.21 \frac{V^{2/5}}{1.5 + \cot \varphi} - 0.75 \quad [3]$$

with an  $R^2$  of 0.44 for the normal stress and 0.58 for the reattachment location. The coefficients have the dimensions  $75.8 \text{ kg/m}^{17/5}$ ,  $156 \text{ N/m}^2$ ,  $6.21 \text{ m}^{1/5}$  and  $0.75 \text{ m}$ . The negative offset is the result of the required conditions for flow separation expressed as a combination of the landward slope steepness and the overtopping volume. These conditions were derived by Van Bergeijk et al. (2022) and indicate that a minimum overtopping volume of  $5 \text{ m}^3/\text{m}$  is required for a steepness of 1:3, while flow separation already occurs for a volume of  $0.75 \text{ m}^3/\text{m}$  for a steepness of 1:1. The reattachment location depends on the overtopping volume. Therefore, the normal stress along the upper slope can be calculated by combining Equations [2] and [3] when the load during a storm with various overtopping volumes is calculated.

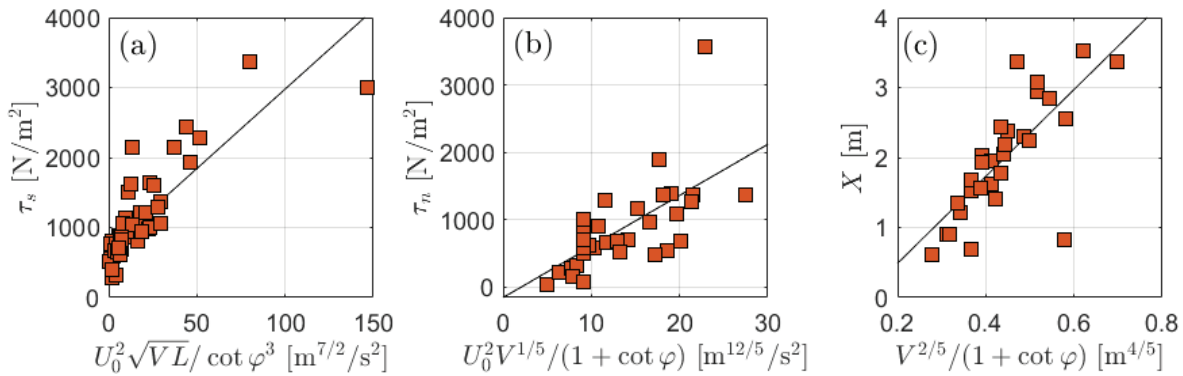


**Figure 5:** The fits for the maximum load at slope changes. (a) the maximum shear stress at the landward toe. (b) the maximum normal stress as result of flow separation at the landward crest line. (c) the location of reattachment measured as the horizontal distance from the crest line.

### 3.2 Height Transitions on The Slope

Height transitions on the slope (Case 2, Figure 3) with a height  $d$  varying between 0.2 and 1 m were simulated. The regression analysis showed that both the shear stress and the normal stress depend similarly on the height of the transitions and the flow velocity before the height transition  $U$  (Figure 6)

$$\tau_{s,height\ slope} = 29.4 d^{1/3} U^2 - 443 \quad [4]$$

$$\tau_{n,height\ slope} = 11.8 d^{1/3} U^2 - 108 \quad [5]$$

with an  $R^2$  of 0.82 for the shear stress and 0.60 for the normal stress. The coefficients have the dimensions  $29.4 \text{ kg/m}^{10/3}$ ,  $443 \text{ N/m}^2$ ,  $11.8 \text{ kg/m}^{10/3}$  and  $108 \text{ N/m}^2$ . The increase in load with increasing height was also found in previous studies (Scheres & Schüttrumpf, 2020; Stanczak, 2008).

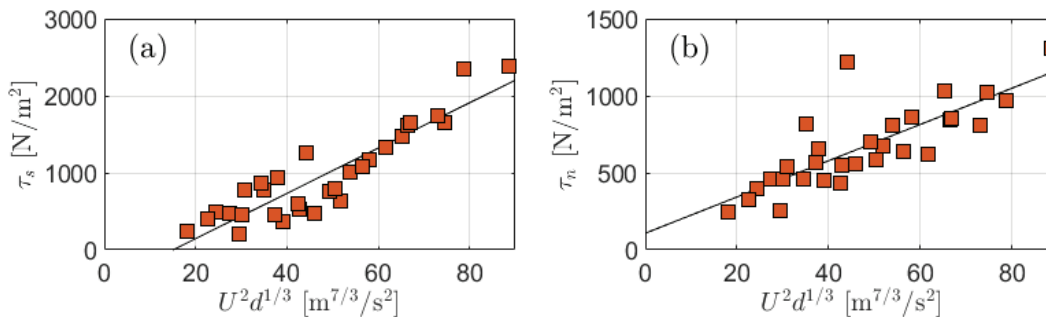


**Figure 6:** The fits for the maximum load at height transitions on the slope. (a) the maximum shear stress. (b) the maximum normal stress.

### 3.3 Height Transitions on The Crest

Transitions with a height  $d$  varying between 5 cm and 25 cm were simulated on the crest. The maximum shear stress and maximum normal stress as the result of height transitions on the crest (Figure 7) show a larger spread compared to the height transitions on the slope (Figure 6). The fits have a smaller  $R^2$  of 0.45 for the shear stress and 0.30 for the normal stress. This is because the height transitions on the crest are a combination of a vertical rise and a vertical drop. The height transitions on the crest show a smaller dependency on the height of transition. A possible explanation is that the maximum stress occurs as result of flow sweeping up into the air due to the vertical rise, and the height that the flow reaches in the air does not strongly depend on the height of the vertical rise.

$$\tau_{s,height\ crest} = 72.1 d^{1/5} U^2 - 196 \quad [6]$$

$$\tau_{n,height\ crest} = 12 d^{1/6} U^2 + 24 \quad [7]$$

The coefficients have the dimensions  $72.1 \text{ kg/m}^{16/5}$ ,  $195 \text{ N/m}^2$ ,  $12 \text{ kg/m}^{19/6}$  and  $24 \text{ N/m}^2$ . Similar to the height transitions on the slope, the load depends on  $U^2$ . Van Doorslaer et al., (2017) found a similar dependency for the impact forces by overtopping waves on a vertical wall, where they showed that the force is proportional to  $U^2$  related to the kinetic energy.

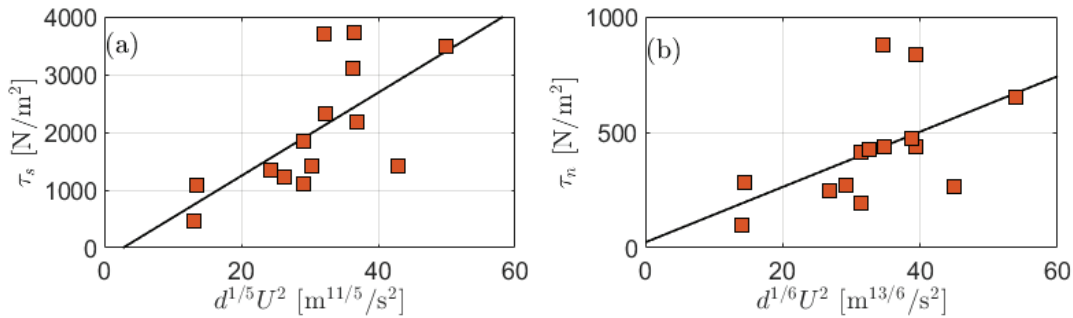


**Figure 7** : The fits for the maximum load at height transitions on the crest. (a) the maximum shear stress. (b) the maximum normal stress.

#### 4. APPLICATIONS

This study shows that geometrical transitions have a larger influence on the hydraulic load due to flow separation and impact. Figure 4 shows that the locations of high hydraulic loads are not at the geometrical transitions, but downstream of these transitions. Therefore, it is important to calculate the hydraulic load along the profile and include the downstream effects of transitions in existing models. This is for example possible in the analytical grass-erosion model GEM (Van Bergeijk et al., 2021) and the wave impact method WIM (Ponsoen et al., 2019). The cumulative overload method COM (Van Der Meer et al., 2010) is currently used in Dutch guidelines and does not yet calculate the hydraulic load along the profile. Since the COM is based on the flow velocity, the COM can be extended using analytical formulas to calculate the flow velocity along the profile (Van Bergeijk et al., 2019; Schüttrumpf & Oumeraci, 2005).

New relations are developed for the hydraulic load of the overtopping flow at geometric transitions. These relations can be used in existing calculation methods for cover failure by overtopping waves to determine the cover erosion during storms (Van Bergeijk et al., 2021; Steendam et al., 2014) or assess the stability of covers (Barendse et al., 2022). For example, the relations can be used as a multiplication factor for the flow velocity in the GEM, WIM or COM. Next to a load description, failure models require a description of the cover strength. Future research into the description of the cover strength is recommended for grass covers as well as innovative covers. The strength of the grass cover is mainly based on overflow experiments (Verheij et al., 1995) or calibration (Steendam et al., 2014). This requires expansive overtopping tests for new and innovative covers such as grass on sandy soils (Van Hoven & Klerk, 2021), grass vegetation on top of block revetments (Van Steeg, 2016) and flower-rich and herb-rich mixtures (Scheres & Schüttrumpf, 2020).

The model results for height transitions can be used to quantify the increase in load as the result of cover erosion. The model results show an increase of the load in the erosion hole and this can lead to an acceleration of the erosion process. Van Bergeijk et al. (2021) showed that damages to the grass cover can increase the failure probability by a factor 4 to 120 depending on the remaining cover strength. The relation for the normal stress and shear stress at height transitions can also be used in models for follow-up erosion mechanisms such as head-cut erosion that describes the deepening and migration of an erosion hole (Van Bergeijk et al., 2021; NRCS, 1997). Klerk et al. (2021) developed a method to combine the GEM and the head-cut erosion model to assess the efficiency of multiple maintenance and inspection schedules. The high hydraulic loads landward of geometrical transitions provide new insights into the maintenance of the covers. The results show that it is not only important to ensure a good quality cover at the transition itself, but more importantly a good quality cover at the location of reattachment.

#### 5. CONCLUSIONS

Geometrical transitions such as slope changes and height differences significantly affect the hydraulic load on the cover by overtopping waves and are therefore important to include in the design and the safety assessment of flood defences. New relations for the hydraulic load are developed for three cases: (1) the slope change at the landward crest line and the slope change at the landward toe, (2) height transitions on the

slope, (3) height transitions on the crest. These relations calculate the maximum shear stress and the maximum normal stress using design parameters such as the geometry and the overtopping volume. These relations can be used to include the effects of geometrical transitions on the hydraulic load in existing calculation methods for cover failure and thereby improve the accuracy of these calculations.

The model results showed that the load is not maximal at the transition, but landward of the transition. This indicates that it is not sufficient to calculate only the load at the transition: the effects of the transitions on the downstream flow need to be considered as well. Moreover, the results show that the hydraulic load as result of a vertical rise is higher compared to the hydraulic load as result of a vertical drop.

The findings in this research are the first step towards understanding the behavior of dike covers under hydrodynamic wave loads. We identified that knowledge about the geotechnical strength of vegetated dike covers is limited. In future studies are working on the transition towards Future-Proof dikes as a nature-based solution, which are safe, are constructed from environmentally friendly local soil with a biodiverse vegetation and are resilient against climate change.

## 6. ACKNOWLEDGEMENTS

This work is part of the research programme All-Risk, with project number P15-21, which is (partly) financed by the Netherlands Organisation for Scientific Research (NWO). Additionally, this work was partly funded by Rijkswaterstaat as part of the EU Interregproject Polder2C's. This work was carried out on the Dutch national e-infrastructure with the support of SURF Cooperative.

## 7. REFERENCES

- Altomare, C., Crespo, A.J.C., Dominguez, J.M., Gómez-Gesteira, M., Suzuki, T., and Verwaest, T. (2015). Applicability of Smoothed Particle Hydrodynamics for estimation of sea wave impact on coastal structures. *Coastal Engineering*, 96, 1–12. <https://doi.org/10.1016/j.coastaleng.2014.11.001>
- Bakker, J.J., Mom, R.J.C., and Steendam, G.J. (2008). *Factual Report: Golfoverslagproeven Zeeuwse zeedijken (in Dutch)*.
- Barendse, L., Van Bergeijk, V.M., Chen, W., Warmink, J.J., Mughal, A., Hill, D., and Hulscher, S.J.M.H. (2022). Hydrodynamic Modelling of Wave Overtopping over a Block-Covered Flood Defence. *Journal of Marine Science and Engineering*, 10(1), 89.
- Bomers, A., Aguilar-López, J.P., Warmink, J.J., and Hulscher, S.J.M.H. (2018). Modelling effects of an asphalt road at a dike crest on dike cover erosion onset during wave overtopping. *Natural Hazards*, 93(1), 1–30.
- Chen, W., Van Gent, M.R.A., Warmink, J.J., and Hulscher, S.J.M.H. (2020). The influence of a berm and roughness on the wave overtopping at dikes. *Coastal Engineering*, 156, 103613.
- Chen, W., Warmink, J.J., Van Gent, M.R.A., and Hulscher, S.J.M.H. (2021). Numerical modelling of wave overtopping at dikes using OpenFOAM®. *Coastal Engineering*, 166.
- Frankena, M. (2019). Modelling the influence of transitions in dikes on grass cover erosion by wave overtopping. *Master Thesis, University of Twente, Water Engineering and Management, Enschede, The Netherlands*.
- Klerk, W.J., Van Bergeijk, V.M., Kanning, W., Wolfert, A.R.M., and Kok, M. (2022). Dealing with shock-based degradation of flood defence systems through inspection, maintenance and structural interventions. *Submitted*.
- NRCS. (1997). Chapter 51 Earth Spillway Erosion Model and Chapter 52 Field Procedures Guide for the Headcut Erodability Index. In *National Engineering Handbook Part 628 Dams*.
- Özer, I.E., Van Damme, M., and Jonkman, S.N. (2020). Towards an International Levee Performance Database (ILPD) and Its Use for Macro-Scale Analysis of Levee Breaches and Failures. *Water 2020, Vol. 12, Page 119, 12(1)*, 119. <https://doi.org/10.3390/W12010119>
- Palma, G., Formentin, S.M., Zanuttigh, B., Contestabile, P., and Vicinanza, D. (2019). Numerical simulations of the hydraulic performance of a breakwater-integrated overtopping wave energy converter. *Journal of Marine Science and Engineering*, 7(2). <https://doi.org/10.3390/jmse7020038>
- Ponsioen, L., van Damme, M., Hofland, B., and Peeters, P. (2019). Relating grass failure on the landside slope to wave overtopping induced excess normal stresses. *Coastal Engineering*, 148, 49–56. <https://doi.org/10.1016/j.coastaleng.2018.12.009>
- Scheres, B., and Schüttrumpf, H. (2020). Investigating the Erosion Resistance of Different Vegetated Surfaces for Ecological Enhancement of Sea Dikes. *Journal of Marine Science and Engineering*, 8(519), 19.
- Schüttrumpf, H., and Oumeraci, H. (2005). Layer thicknesses and velocities of wave overtopping flow at seadikes. *Coastal Engineering*, 52(6), 473–495. <https://doi.org/10.1016/j.coastaleng.2005.02.002>
- Simm, J., Ballard, B.W., Flikweert, J.J., Van Maren, E., Dimakopoulos, A., Kinnear, R., Arthur, M., Tourment, R., Neutz, C., and Van Steeg, P. (2021). Investigation, assessment and remediation of levee transitions. *FLOODrisk 2020 - 4th European Conference on Flood Risk Management*.

- Stanczak, G. (2008). Breaching of Sea Dikes Initiated from the Seaside by Breaking Wave Impacts. *PhD Thesis, University of Braunschweig, Faculty of Architecture, Civil Engineering and Environmental Sciences, and University of Florence, Faculty of Engineering.*
- Steendam, G.J., Van Hoven, A., Van der Meer, J.W., and Hoffmans, G. (2014). Wave Overtopping Simulator Tests on Transitions and Obstacles At Grass-covered Slopes of Dikes. *Coastal Engineering Proceedings*, 1(34). <https://doi.org/10.9753/icce.v34.structures.79>
- Talukdar, P., and Dey, A. (2019). Hydraulic failures of earthen dams and embankments. *Innovative Infrastructure Solutions*, 4(1), 1–20.
- Van Bergeijk, V.M. (2022). Over the Dike Top: Modelling the Hydraulic Load of Overtopping Waves including Transitions for Dike Cover Erosion. *PhD Thesis University of Twente, Water Engineering and Management, Enschede, The Netherlands.*
- Van Bergeijk, V.M., Verdonk, V.A., Warmink, J.J., and Hulscher, S.J.M.H. (2021). The Cross-Dike Failure Probability by Wave Overtopping over Grass-Covered and Damaged Dikes. *Water*, 13(5), 690. <https://doi.org/10.3390/w13050690>
- Van Bergeijk, V.M., Warmink, J.J., and Hulscher, S.J.M.H. (2022). The wave overtopping load on landward slopes of grass-covered flood defences: Deriving practical formulations using a numerical model. *Coastal Engineering*, 171(104047). <https://doi.org/10.1016/j.coastaleng.2021.104047>
- Van Bergeijk, V.M., Warmink, J.J., Van Gent, M.R.A., and Hulscher, S.J.M.H. (2019). An analytical model of wave overtopping flow velocities on dike crests and landward slopes. *Coastal Engineering*, 149, 28–38. <https://doi.org/10.1016/j.coastaleng.2019.03.001>
- Van Bergeijk, V.M., Warmink, J.J., and Hulscher, S.J.M.H. (2020a). Modelling the Wave Overtopping Flow over the Crest and the Landward Slope of Grass-Covered Flood Defences. *Journal of Marine Science and Engineering*, 8(7), 489. <https://doi.org/10.3390/jmse8070489>
- Van Bergeijk, V.M., Warmink, J.J., and Hulscher, S.J.M.H. (2021). *Experimental set-up and modelling tools for the load by overtopping waves in erosion models.*
- Van Bergeijk, V.M., Warmink, J.J., and Hulscher, S.J.M.H. (2020b). Modelling of Wave Overtopping Flow over Complex Dike Geometries: Case Study of the Afsluitdijk. *Coastal Engineering Proceedings*, 1–9. <https://doi.org/10.9753/icce.v36v.papers.52>
- Van Damme, M., Ponsioen, L., Herrero, M., and Peeters, P. (2016). Comparing overflow and wave-overtopping induced breach initiation mechanisms in an embankment breach experiment. *E3S Web of Conferences*, 7, 1–9. <https://doi.org/10.1051/e3sconf/20160703004>
- Van Der Meer, J.W., Hardeman, B., Steendam, G.J., Schüttrumpf, H., and Verheij, H. (2010). Flow depths and velocities at crest and landward slope of a dike, in theory and with the wave overtopping simulator. *Coastal Engineering Proceedings*, 1(32), 10.
- Van Doorslaer, K., Romano, A., De Rouck, J., and Kortenhuis, A. (2017). Impacts on a storm wall caused by non-breaking waves overtopping a smooth dike slope. *Coastal Engineering*, 120, 93–111. <https://doi.org/10.1016/J.COASTALENG.2016.11.010>
- Van Hoven, A., and Klerk, W.J. (2021). Gras op zand onderzoek product 8: Analyse golfklapproeven en golfoverslagproeven (in Dutch). In *11204369-002-GEO-0015*.
- Van Steeg, P. (2016). *Stabiliteit taludbekleding van Hillblock 2.0, Drainageblock en Grassblock: Grootschalig modelonderzoek in Deltagoot (in Dutch).*
- Verheij, H.J., Meijer, D.G., Kruse, G.A.M., Smith, G.M., and Vesseur, M. (1995). *Investigation of the strength of a grass cover upon river dikes.*
- Zhang, Y., Chen, G., Hu, J., Chen, X., Yang, W., Tao, A., and Zheng, J. (2017). Experimental study on mechanism of sea-dike failure due to wave overtopping. *Applied Ocean Research*, 68, 171–181. <https://doi.org/10.1016/j.apor.2017.08.009>